Research Paper

Mitochonic Acid 5 (MA-5) Facilitates ATP Synthase Oligomerization and Cell Survival in Various Mitochondrial Diseases

Tetsuro Matsuhashi [a,1], Takeya Sato [b,1], Shin-ichiro Kanno [c,1], Takehiro Suzuki [d,e,1], Akihiro Matsuo [d], Yuki Oba [d], Motoi Kikusato [f], Emi Ogasawara [g], Tai Kudo [h], Kosuke Suzuki [d], Osamu Ohara [i], Hiroko Shimbo [j], Fumika Nanto [d], Hiroaki Yamaguchi [k], Daisuke Saigusa [l], Yasuno Mukaiyama [d], Akiko Watabe [m], Koichi Kikuchi [d], Hisato Shima [d], Eikan Mishima [d], Yasutoshi Akiyama [d], Yoshitsugu Oikawa [a], Hsin-Jung HO [d,e], Yukako Akiyama [d], Chitose Suzuki [d], Mitsugu Uematsu [a], Masaki Ogata [n], Naonori Kumagai [a], Masaaki Toyomizu [f], Atsushi Hozawa [l], Nariyasu Mano [k], Yuji Owada [n], Setsuya Aiba [m], Teruyuki Yanagisawa [b], Yoshihisa Tomioka [o], Shigeo Kure [a], Sadayoshi Ito [d], Kazuto Nakada [g], Ken-ichiro Hayashi [p], Hitoshi Osaka [q], Takaaki Abe [d,e,r,*]

[a] Department of Pediatrics, Tohoku University Graduate School of Medicine, Sendai 980-8574, Japan
[b] Department of Molecular Pharmacology, Tohoku University Graduate School of Medicine, Sendai 980-8574, Japan
[c] Division of Dynamic Proteome in Cancer and Aging, Institute of Development, Aging and Cancer, Tohoku University, Sendai 980-8574, Japan
[d] Division of Nephrology, Endocrinology and Vascular Medicine, Tohoku University Graduate School of Medicine, Sendai 980-8574, Japan
[e] Department of Medical Science, Tohoku University Graduate School of Biomedical Engineering, Sendai 980-8574, Japan
[f] Animal Nutrition, Life Sciences, Graduate School of Agricultural Science, Tohoku University, Sendai 981-8555, Japan
[g] Faculty of Life and Environmental Science, University of Tsukuba, Ibaraki 305-8572, Japan
[h] Primetech Co. Ltd., Tokyo, 112-0002, Japan
[i] Kazusa DNA Research Institute, Kisarazu, 292-0818, Japan
[j] Kanagawa Children's Medical Center, Yokohama 232-0066, Japan
[k] Department of Pharmaceutical Sciences, Tohoku University Hospital, Sendai 980-8574, Japan
[l] Department of Medical Megabank, Tohoku University, Sendai 980-8574, Japan
[m] Division of Dermatology, Tohoku University Graduate School of Medicine, Sendai 980-8574, Japan
[n] Department of Organ Anatomy, Tohoku University Graduate School of Medicine, Sendai 980-8574, Japan
[o] Laboratory of Oncology, Pharmacy Practice and Sciences, Tohoku University Graduate School of Pharmaceutical Sciences, Sendai, Japan
[p] Department of Biochemistry, Okayama University of Science, Okayama 700-0005, Japan
[q] Division of Pediatrics, Jichi Medical University, Shimotsuke, 329-0498, Japan
[r] Department of Clinical Biology and Hormonal Regulation, Tohoku University Graduate School of Medicine, Sendai 980-8574, Japan

A R T I C L E   I N F O

A B S T R A C T

Mitochondrial dysfunction increases oxidative stress and depletes ATP in a variety of disorders. Several antioxidant therapies and drugs affecting mitochondrial biogenesis are undergoing investigation, although not all of them have demonstrated favorable effects in the clinic. We recently reported a therapeutic mitochondrial drug mitochonic acid MA-5 (Tohoku J. Exp. Med., 2015). MA-5 increased ATP, rescued mitochondrial disease fibroblasts and prolonged the life span of the disease model "Mitomouse" (JASN, 2016). To investigate the potential of MA-5 on various mitochondrial diseases, we collected 25 cases of fibroblasts from various genetic mutations and cell protective effect of MA-5 and the ATP producing mechanism was examined. 24 out of the 25 patient fibroblasts (96%) were responded to MA-5. Under oxidative stress condition, the GDF-15 was increased and this increase was significantly abrogated by MA-5. The serum GDF-15 elevated in Mitomouse was likewise reduced by MA-5. MA-5 facilitates mitochondrial ATP production and reduces ROS independent of ETC by facilitating ATP synthase oligomerization and supercomplex formation with mitofilin/Mic60. MA-5 reduced mitochondria

fragmentation, restores crista shape and dynamics. MA-5 has potential as a drug for the treatment of various mitochondrial diseases. The diagnostic use of GDF-15 will be also useful in a forthcoming MA-5 clinical trial.

1. Introduction

Mitochondrial diseases are life-threatening and progressive because of increased oxidative stress and depleted ATP are serious problems that can cause cell death (Schapira, 2012; Vafai and Mootha, 2012).

However, they are largely untreatable because of the lack of effective drugs (Avula et al., 2014; Gorman et al., 2016). Recently, we invented and reported a mitochondria-homing drug, Mitochonic acid-5 (MA-5) (4-(2,4-difluorophenyl)-2-(1H-indole-3-yl)-4-oxobutanoic acid), that both increases cellular ATP and protects mitochondrial patients' fibroblasts from cell death (Suzuki et al., 2015, 2016). MA-5 also upregulated cardiac and renal respiration in the mitochondrial disease model Mitomouse (Nakada et al., 2001), resulting in a prolongation of survival (Suzuki et al., 2016). In the reports, we examined the effect of MA-5 in one case each of Leigh syndrome, myopathy encephalopathy lactic acidosis and stroke-like episodes (MELAS), Kearns-Sayre syndrome (KSS) and Leber hereditary optic neuropathy (LHON) patient fibroblasts. However, within the mitochondrial diseases, there are many gene mutations of electron transfer complex (ETC) and ATP synthase that have a deleterious impact on their functions (Koopman et al., 2012). Therefore, the aim of this study is to examine the general effectiveness of MA-5 across a range of mitochondrial disease fibroblasts with a variety of genetic mutations. In addition, for designing a clinical study of a drug, effective biomarkers are necessary to enable the selection of responsive participants, optimization of the dosing regimens and assessment of the treatment efficacy (Hurko, 2013). Recently, it was reported that growth differential factor 15 (GDF-15) may be an effective marker of mitochondrial damage and thus useful in the diagnosis of mitochondrial diseases (Fujita et al., 2014; Yatsuga et al., 2015). However, the relation between therapeutic intervention and the GDF-15 level has not been well determined. We therefore examined the GDF-15 level when mitochondria have being damaged by oxidative stress and whether it would be reduced by MA-5. We also examined the effectiveness of GDF-15 as a therapeutic marker in a mitochondrial disease model "Mitomouse". In our previous report, MA-5 was shown to increase the cellular ATP level with the mechanism apparently carried out by its mitochondrial membrane binding protein, mitofilin/Mic60 (Suzuki et al., 2016, 2015). However, the precise mechanism underlying the increase in ATP has not been elucidated yet. To identify the mechanism of action of MA-5, we examined the bioenergetic analysis of mitochondria and examined the formation of a supercomplex of ATP synthase with mitofilin/Mic60. Because energetic change of mitochondria has a potent influence on mitochondrial morphology and kinetics (Giedt et al., 2012; Kumari et al., 2016), we also evaluated the shape and movement of mitochondria with or without MA-5 in patient fibroblasts.

2. Materials and Methods

2.1. Synthesis of MA-5

MA-5, 4-(2,4-difluorophenyl)-2-(1H-indole-3-yl)-4-oxobutanoic acid was chemically synthesized at Okayama University of Science as previously reported (Suzuki et al., 2015). BSO (L-Buthionine-(S,R)-sulfoximine was purchased from Wako Pure Chemical Industries).

2.2. Human Skin Fibroblasts

Fibroblasts obtained by skin biopsy of mitochondrial disease patients were collected in Kanagawa Children's Medical Center (KCMC),

Jichi Medical University and Tohoku University Hospital under the approval of the Ethical Committee of Tohoku University. Written informed consent was obtained from all of the patients.

Among 25 mitochondrial disease cases we examined, case 5 (Leigh), case 11 (MELAS), case 17 (LHON) and case 20 (KSS) are examined as previous reported (Suzuki et al., 2015). In the cell viability experiments, fibroblasts were cultured in 1.0 g/L low-glucose DMEM with 10% FBS at 37 °C in 5% CO_2. Cell viability assay was performed (Suzuki et al., 2015). The LDH level was measured by cell count using LDH cytotoxicity detection kit (Takara). The levels of GDF-15 and FGF-21 were determined using a Quantikine Human GDF-15 ELISA Kit and Quantikine Human FGF-21 ELISA Kit (R&D Systems), respectively.

2.3. Measurement of Heteroplasmy Levels of Mitochondrial DNA Mutations

The mitochondrial DNA mutation heteroplasmy level was examined by deep sequencing of the mutated regions. The primers used for amplification of the target regions of each patient fibroblast are listed in Supplementary Table 1. After the first PCR amplification, the PCR products were subjected to the second-round PCR for attachment of the index sequences required for next-generation DNA sequencing on an illumine NextSeq500 sequencer (Illumina Inc.) as described previously (Shimbo et al., 2014; Nakayama et al., 2017). The PCR products were read on a 150-base paired-end mode. The number of reads containing a mutation of interest was counted using a combination of bioinformatics tools (BWA, 0.7.15; Picard, 2.8.2; GATK, 3.7; https://software.broadinstitute.org/gatk/). The heteroplasmy was expressed as a ratio of the read number with mutation over the total read number ($>10^5$ reads) in percentage terms. We also examined the heteroplasmy level by PCR-RFLP analysis (Supplementary Fig. 1, according the Supplementary Methods) and primers used for PCR is listed in Supplementary Table 2.

2.4. Mitomouse

All animal experiments were approved by Tohoku University and Tsukuba University Animal Care Committees. Mitomouse carrying wild-type mtDNA and mutant mtDNA with a pathogenic 4696-bp deletion was generated by our group (Nakada et al., 2001). Mitomouse were fed with normal chow and MA-5 at 50 mg/kg body weight per day or the vehicle corn oil for 30 days. The GDF-15 level in the Mitomouse was measured with a Quantikine Mouse/Rat GDF-15 ELISA Kit (R&D Systems).

2.5. Mitochondrial Function Measurement

The oxygen consumption and pH gradient of the fibroblasts from the Leigh patients or normal volunteers were measured using Seahorse XF 24 (Seahorse Bioscience). Briefly, cells were cultured in the assay medium (70 mM sucrose, 220 mM mannitol, 10 mM KH_2PO_4, 5 mM $MgCl_2$, 2 mM HEPES, 1.0 mM EGTA and 0.2% (w/v) fatty acid-free BSA, pH 7.2) without CO_2 for 60 min, then, after equilibration, cells were measured in the three respiration rates followed by injections of three inhibitors of mitochondrial oxidative phosphorylation (OXPHOS)

2.6. Membrane Potential Analysis of Mitochondrial Membrane

The membrane potential of mitochondria was measured with a Mito-ID™ membrane potential Cytotoxicity Kit (Enzo Life Science).

2.7. The Measurement of ATP Production After Treatment with DMSO or MA-5

Fibroblasts from a Leigh syndrome patient (Fig. 3e, left panel, Case 10 in Table 1) and a MELAS patient (Fig. 3e, right panel, Case 15 in Table 1) were cultured in 96 well plates at 3000 cells per each well (n = 4). The ATP level was measured 3 h after DMSO or MA-5 treatment (10 μM) by ATP measurement kit (Toyo ink).

2.8. Blue-Native (BN) and Clear-Native (CN) PAGE

30 μg of bovine heart mitochondria were solubilized with 50 μL of phospholipids buffer, following DMSO (0.1%) or MA-5 (100 μM) treatment for 30 min on ice.

After 20 min of centrifugation at 17,400 rpm at 4 °C, the pellet of mitochondria was dissolved by 30 μL of 0.25%, 0.5% and 1% digitonin with 7.5 μL of Native Page sample buffer. After electrophoresis, the CN-PAGE gel was incubated in pre-incubation buffer (270 mM Glycine and 35 mM Tris/HCl, pH 7.4) for 2 h at 37 °C. Then the gel was incubated in assay buffer (35 mM Tris, 270 mM Glycine, 14 mM $MgSO_4$, 0.2% $Pb(NO_3)_2$, 8 mM ATP, pH 8.3) at 37 °C. ATP hydrolysis correlated with the development of a white lead phosphate precipitate (Strauss et al., 2008). For Western blot, the BN-PAGE gel was transferred to a PVDF membrane. The membrane was incubated with the antibodies ATP5A (ab110271, Abcam), ATP5B (ab14730, Abcam), ATP5I (16483-1-AP, Proteintech, Japan), ATP5L (16307-1-AP, Proteintech) and mitofilin (ab137057, Abcam), and the bands were detected using the enhanced Chemiluminescent plus system (Amersham). We confirmed the protein loading level in each lane by Western blot using VDAC1 (Abcam, ab18988) as an internal protein marker. In addition, the same amount of mitochondria used for BN-PAGE was solubilized with 1.0% digitonin, then electrophoresed using SDS-PAGE, and western blotting was performed with VDAC 1 antibody (ab18988, Abcam) as the loading control. The concentration ratio of each monomer or dimer band of ATP5A was measured using ImageJ software, and statistical analysis was performed as shown in Fig. 4c.

2.9. Mass Spectrometry Analysis

Eluted proteins were separated on 4–12% gradient BN–PAGE gels (Invitrogen) and stained with Silver. Each gel lane was cut into gel slices, and the proteins therein were in-gel digested with trypsin (Promega). MALDI-TOF MS was carried out on a Voyager-De-Pro Biospectrometry Workstation (Applied Biosystems). Mass spectra were collected in positive reflectron mode in a mass range between 700 and 4000 Da. Peptide masses were matched against the Swiss-Prot, NCBInr, and MSDB databases using the MASCOTsearch engine (Matrix Sciences) with a 100 ppm mass tolerance error.

2.10. Immunoprecipitation of Mitofilin/Mic60 Binding Proteins

The HEK293 cells stably expressing Flag-IMMT generated by Flip-in T-Rex system (1 mL) and the control cells (generated by pcDNA5/FRT/TO vector only) (1 mL) were homogenized in SHE buffer (10 mM Hepes pH 7.4, 0.21 M mannitol, 0.07 M sucrose, 0.1 M EDTA, 0.1 M EGTA, 0.15 mM spermine, 0.75 mM spermidine) and centrifuged for 10 min at 3000 rpm. The pellets were rinsed with SHE buffer and centrifuged once more. The pellets were then extracted in 1 mL of extraction buffer (50 mM HEPES pH 7.4, 0.3 M NaCl, 0.2% NP40) by sonication and the extracts were clarified by centrifugation at 12,000 rpm for 30 min at

Table 1
The characteristics and MA-5 response in skin fibroblasts from patients with mitochondrial diseases.
#1 Shimbo H. et al., Mol. Genet. Metab. Rep. 1: 33, 2014.

Case	Disease	Age	Cell ID	Gene mutation	Protein	Sensitivity for BSO	Effect of MA-5	GDF-15 (pg/mL)	FGF-21 (pg/mL)	Mutation rate (%) NGS	RFLP
1	Leigh	8	THK2	m.10191T>C	ND3	(+)	(+)	4555.7	3230		
2	Leigh	16	THK5	(−)	(−)	(+)	(+)				
3	Leigh	8	THK6	m.10191T>C	ND3	(+)	(+)	2051.5	3241.8	17	
4	Leigh	16	THK7	(−)	(−)	(+)	(+)	1072.4	732.8		
5	Leigh	0	KCMC10	m.10158T>C	ND3	(+)	(+)			82	87.9
6	Leigh	5	KCMC14	m.8993T>G	ATPase6	(+)	(+)				
7	Leigh	2	KCMC15	p.Ala248Asp	SURF1	(+)	(+)			78[#1]	
8	Leigh	0.8	KCMC17	c.367_368del AG	SURF1	(+)	(+)				
9	Leigh	5	ME54−1	c.55C>T	NDUFA1	(+)	(+)	671.2	149.2		
10	Leigh	34	THK17	(−)	(−)	(+)	(+)	1033.7	1192.7		
11	MELAS	14	KCMC9	m.3243A>G	tRNA-Leu	(+)	(+)			21	17.2
12	MELAS	14	KCMC11	m.3243A>T	tRNA-Leu	(+)	(+)			38	49.4
13	MELAS	13	KCMC12	m.586G>A	tRNA-Phe	(+)	(+)				
14	MELAS	56	THK12	m.3243A>G	tRNA-Leu	(+)	(+)	5505.7	1708.1	81	85.4
15	MELAS	20	THK28	m.3243 A>G	tRNA-Leu	(+)	(+)	1929.7	784.8	48	49
16	MELAS	9	ME07−1	m.4450G>A	tRNA-Met	(+)	(+)	784.5	205.8		
17	LHON	18	THK8	m.11778G>A	ND4	(+)	(+)	520.1	80.9	100	100
18	LHON	66	THK9	m.11778G>A	ND4	(−)	(−)	2647	434.9	100	100
19	LHON	41	THK10	m.11778G>A	ND4	(+)	(+)	1322.4	912.1	97	82
20	KSS	13	THK4	(−)	(−)	(+)	(+)	2900.2	2088.5		
21	CPEO	15	THK23	(−)	(−)	(+)	(+)	2461.7	790.8		
22	DOA	73	THK14	c.1377_1381 delTGTAA	p.Asn459Met	(+)	(+)	1310.2	215.8		
23	Unclassified	13	THK1	(−)	(−)	(+)	(+)	4910	789.9		
24	Unclassified	3	THK3	(−)	(−)	(+)	(+)	1071.4	66.5		
25	Unclassified	64	THK11	(−)	(−)	(+)	(+)	4428	396.4		
	Normal	0	THK0	(−)	(−)	(−)	(−)				

Table shows the character of mitochondrial disease patients and the results of the cell viability assay using skin fibroblasts with mitochondrial diseases. In 24 out of 25 (96%) cases of various mitochondrial diseases, MA-5 exhibited a cell-protective effect under the conditions of oxidative stress induced by BSO treatment. One case of LHON was insensitive to BSO (case 18). This case had the same mutation as the other two cases of LHON but was insensitive to BSO, so we were unable to assess the effect of MA-5 on the fibroblasts. The mitochondrial heteroplasmy rate of each case was analyzed by NGS and PCR-RFLP. All the fibroblast assay in this table was performed under 12 passages.
THK, Tohoku University hospital; KCMC, Kanagawa Children's Medical Center; ME, Jichi Medical University Children's Medical Center; MELAS, Mitochondrial myopathy, Encephalopathy, Lactic Acidosis, Stroke-like episodes; LHON, Leber Hereditary Optic Neuropathy; KSS, Kearns-Sayre syndrome; CPEO, Chronic progressive external ophthalmoplegia, DOA, Domestic optic atrophy.
The rate of mutation in Case 7 was reported previously (Shimbo et al., 2014).

4 °C. The nuclear extracts were incubated with anti-flag antibody M2 beads for 4 h in the presence of RNase A (10 mg/mL) and DNase I (10 mg/mL) at 4 °C. After washing three times with washing buffer (0.15 M NaCl, 0.1% NP-40, 50 mM HEPES pH 7.4) and once with PBS, the binding proteins were eluted by 40 mL of 0.1 M glycine buffer pH 3.0. The elutes were neutralized by 1 M Tris-HCl buffer pH 9.5 and suspended in SDS-PAGE sample buffer. The samples were boiled for 5 min and were resolved by SDS-PAGE. The gel was stained using a Wako Mass silver stain kit. Gel slippage was reduced by 100 mM of DTT and alkylated by 100 mM idoacetamide. After washing, the gels were incubated with trypsin overnight at 30 °C. Recovered peptides were desalted by Ziptip c18 (Millipore). Samples were analyzed by nanoLC/MS/MS systems (DiNa HPLC system KYA TECH Corporation/ QSTAR XL Applied Biosystems). Mass data acquisitions were piloted by Mascot software.

2.11. Elution Profile of on Size-Exclusion Chromatography

MA-5 treatment (10 μM, 1 h) and untreated HEC293T cell extracts were separated on a Superose™ 6 (GE Healthcare). The proteins of each fraction were then separated by SDS-PAGE and analyzed by Western blotting with an anti-mitofilin/Mic60 antibody and anti-ATP5A antibody. The Superose™ 6 column was calibrated by the standard proteins (Thyroglobulin 669 kDa, β-amylase 200 kDa, carbonic anhydrase 29 kDa) and Blue dextran (2,000,000 kDa).

2.12. Microscopic Imaging

For live-cell imaging microscopy, culture dishes with fibroblasts from Leigh syndrome patient following Mitotracker (green) staining were placed into a LSM780 Zeiss confocal microscopy system equipped with incubation system S (Carl Zeiss). ZEN2012 software (Carl Zeiss) was used to analyze the trajectory of each mitochondrion.

For super resolution images, cells from a Leigh syndrome patient were stained with MitoRed (shown in red) and the nucleus counterstained with Hoechst3342 (shown in blue). The samples were then placed into a Nikon N-SIM super resolution microscopy system (Nikon). Images were acquired and the data analyzed using NIS-Elements with N-SIM analysis software (Nikon). Electron microscopic analysis was performed as previously reported (Ogata et al., 2015).

2.13. Statistical Analysis

The data are expressed as means ± SEM. Comparisons were made using unpaired two-tailed Student's t-tests, two-way ANOVA and Tukey-Kramer test, as appropriate (JMP Pro 12 software). In the comparison of GDF-15 in the Mitomouse, non-parametric Wilcoxon rank sum test was used. A p value of <0.05 was considered significant ($^{\#}p < 0.05$, $^{\#\#}p < 0.01$, $^{\#\#\#}p < 0.001$, $^{*}p < 0.05$, $^{**}p < 0.01$, $^{***}p < 0.001$).

3. Results

3.1. Cell-Protective Effect of MA-5 Independent of Their Genetic Backgrounds

We have reported that MA-5, a newly synthesized derivative of the plant hormone indole acetic acid, improved the cell survival of fibroblasts from 4 patients with Leigh syndrome, MELAS, LHON and KSS (Suzuki et al., 2015). However, mitochondrial diseases are composed of a heterogeneous group of genetic mutations encoded by either nuclear or mitochondrial DNA (Pieczenik and Neustadt, 2007; Vafai and Mootha, 2012). This heterogeneity hampers both diagnosis and treatment. To evaluate the general efficacy of MA-5 in various mitochondrial diseases, we collected 25 fibroblasts from various mitochondrial disease patients with a wide variety of genetic backgrounds (Table 1). Recently, we (Suzuki et al., 2015) and another group (Enns et al., 2012) reported

that the evaluation of cell viability using a glutathione synthesis inhibitor L-buthionine-(S,R)-sulfoximine (BSO), which reduces glutathione synthesis and increases the ROS level so as to result apoptosis and cell death, is a useful method for evaluating mitochondrial damage in mitochondrial disease patient fibroblasts. In addition, we measured the LDH level in the culture medium to further determine the cell viability. At first, we checked the effect of BSO in normal fibroblasts. In normal skin fibroblasts, the cell viability was unaffected but the LDH level was significantly increased, suggesting mitochondrial damage. This elevated LDH level was reduced by MA-5 in a dose-dependent manner (Supplementary Fig. S1a). In patient fibroblasts, 24 of 25 cases (96%) were sensitive to BSO and responded to MA-5 irrespective of their genetic backgrounds (Table 1). All of the Leigh (10 cases, Fig. 1a and Supplementary Fig. S1b–k) and MELAS patient fibroblasts (6 cases, Fig. 1b and Supplementary Fig. S1l–q) were sensitive to BSO, and MA-5 protected against BSO-induced cell death in a dose-dependent manner. Reciprocally, the LDH level of BSO-treated patient fibroblasts was significantly increased and this BSO-induced increase was abrogated by MA-5. In 3 cases of LHON, 2 cases were sensitive to BSO and that MA-5 protected against cell death (Fig. 1c and Supplementary Fig. S1r–t). MA-5 was ineffective in the other case of LHON (Case 18). This case had the same mutation as the other two cases of LHON but was insensitive to BSO, so we were unable to assess the effect of MA-5 on the fibroblasts. We found that all the rest of the 6 cases (1 each case of KSS, DOA and chronic progressive external ophthalmoplegia (CPEO), and 3 cases of genetically unidentified mitochondrial diseases) were also sensitive to BSO and MA-5 protected against cell death (Supplementary Fig. S1u–z). These data suggest that MA-5 induces a cell-protective effect independently of the genetic background in a variety of mitochondrial diseases. We also examined the mitochondrial DNA heteroplasmy levels. Among 25 cases, 13 cases have affected mitochondrial DNA mutation and we can confirm heteroplasmy level of 10 cases and mentioned in Table 1 and Supplementary Fig. S2. The heteroplasmy level was varied at 15–97%.

3.2. GDF-15 Predicts MA-5-Responsiveness and Prognosis

When planning a clinical study with a drug fist-in-human, effective biomarkers enable the selection of responsive participants, optimization of the dosing regimens and assessment of the efficacy of the drug (Hurko, 2013). In mitochondrial diseases, the lactate to pyruvate (L/P) ratio, FGF-21 (Suomalainen et al., 2011) and GDF-15 (Suomalainen et al., 2011; Yatsuga et al., 2015) are candidates for diagnosing and evaluating the progression in mitochondrial diseases. We measured the serum level of GDF-15 and FGF-21 in 17 available patients with mitochondrial diseases. The average serum concentration of GDF-15 was 2063.26 ± 392.53 pg/mL, representing a significant increase compared with normal volunteers (Fig. 2a, left). The serum levels of FGF-21 in 17 patients with mitochondrial diseases were 1001.24 ± 252.40 pg/mL, with many values overlapping those of normal volunteers (Fig. 2a, right). In addition, there was no significant correlation between the GDF-15 level and FGF-21 level, suggesting that GDF-15 is a better marker for predicting the mitochondrial condition in our patients examined (Fig. 2b).

We next measured the GDF-15 and FGF-21 levels in the culture medium of fibroblasts from patients to further evaluate whether GDF-15 is an effective marker for estimating the mitochondrial damage. The GDF-15 level was significantly increased by BSO in relationship with the exposure time and was significantly increased at 72 h (Fig. 2c). In contrast, FGF-21 was unchanged. We next examined the relationship between the cell-protective effect of MA-5 and the level of GDF-15. In normal fibroblasts, the cell viability was not changed by BSO treatment but the level of GDF-15 in the culture medium was significantly increased, suggesting incipient mitochondrial damage (Fig. 2d). This BSO-induced elevation of GDF-15 in normal fibroblasts was normalized by MA-5. Subsequently, we also measured the GDF-15 in the culture medium of
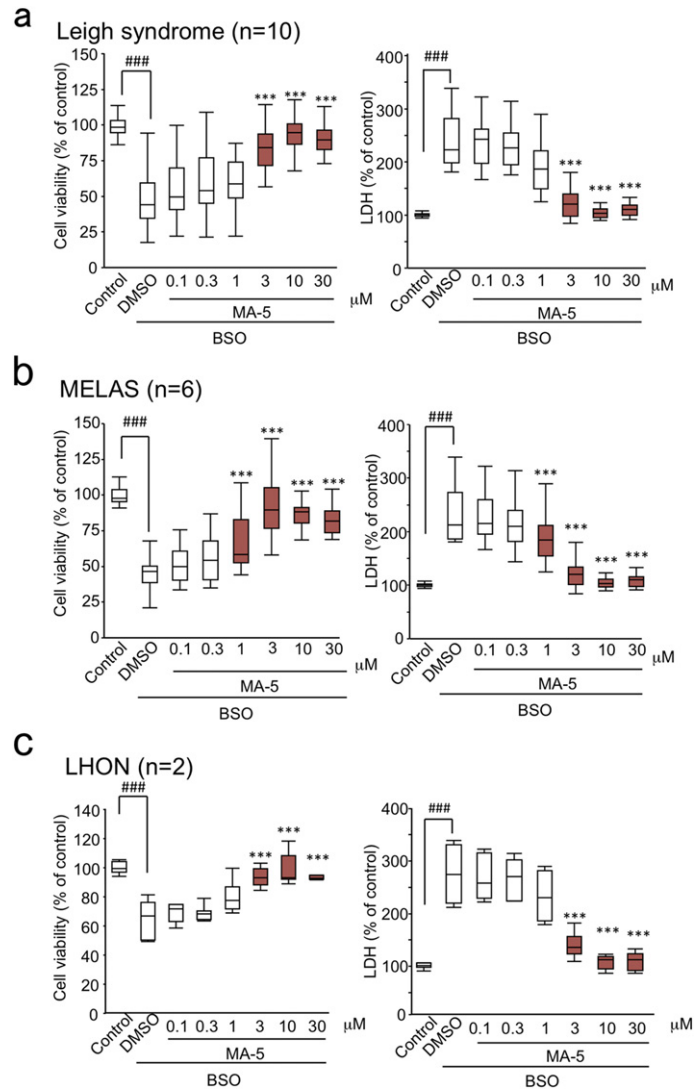
Fig. 1. Cell-protective effect of MA-5 in Leigh syndrome, MELAS and LHON as measured by cell viability assay and the level of LDH in the culture medium. (a) A summary of 10 cases of Leigh syndrome (from case 1 to case 10 in Table 1). (b) A summary of 6 cases of MELAS (from case 11 to case 16 in Table 1). (c) A summary of 2 cases of LHON (case 17 and 19 in Table 1; $n = 2$). MA-5 exerted a cell protective effect against oxidative stress in a dose-dependent manner (MA-5 concentration is from 0.1 to 30 μM). The figure on the left is the cell viability assay and on the right the level of LDH in the culture medium ($n = 10$). The data represent the mean + SEM. ###$p < 0.001$ (two-way ANOVA and Tukey post hoc test versus Control), ***$p < 0.001$ (two-way ANOVA and Tukey–Kramer test versus BSO with DMSO). The red square indicates significantly increased or decreased compared with DMSO.

25 patient fibroblasts with or without BSO (Supplementary Fig. S3a–y). We chose a BSO concentration that reduced the cell survival to approximately 50%. The GDF-15 level was clearly increased by BSO treatment and MA-5 significantly decreased the up-regulated GDF-15 level in the fibroblasts from Leigh syndrome (7 of 10 cases, Fig. 2e), MELAS (5 of 6 cases, Fig. 2f), LHON (2 of 3 cases, Fig. 2g), KSS (1 of 1 case), DOA (1 of 1 case), CPEO (1 of 1 case) and unidentified mitochondria disease (3 of 3 cases). These data further suggest that the GDF-15 level is a useful biomarker that predicts the cell protective effect of MA-5.

3.3. MA-5 Reduced GDF-15 Level in the Mitomouse

Recently, we reported that MA-5 improved the cardiac and renal respiration and prolonged survival in the "Mitomouse", an animal carrying a deleted mitochondrial DNA mutation that which show abnormalities of cardiac conduction system, extraocular muscle paralysis, retinitis pigmentosa, and severe renal failure, partly similar to Kerns-Sayre syndrome (Nakada et al., 2001; Suzuki et al., 2016).

Recently, there are several reports that GDF-15 may be an effective marker of mitochondrial damage and thus useful in the diagnosis of mitochondrial diseases (Fujita et al., 2014; Yatsuga et al., 2015), but the relation between therapeutic intervention and the GDF-15 level has not been well determined and reported. Therefore, we measured the serum level of GDF-15 in the control or MA-5-treated Mitomouse. Before treatment, we confirmed that the genomic mutation rate in the tail was at the same level (~50%) and the serum pyruvate level was increased in all of the Mitomouse. The average level of GDF-15 in Mitomouse was 1064.3 ± 391.8 pg/mL in DMSO group and 919.4 ± 391.8 pg/mL in DMSO group (there was no statistically difference) that is significantly high compared to the normal mouse (77.0 ± 25.24 pg/mL, according the instruction), suggesting the pathologic condition of the Mitomouse.

In the control group ($n = 11$), the GDF-15 level was increased in 8 mice (72.7%) and decreased in 3 mice (27.3%) (Fig. 2h, left). In the MA-5 treatment group ($n = 17$), the GDF-15 was increased in 6 mice (35.3%) and decreased in 11 mice (64.7%), indicating that MA-5-treatment significantly decreased the GDF-15 level compared with the control (Fig. 2h, $p = 0.0369$). These data further suggest that MA-5 works not only in vitro but also in vivo and that GDF-15 could be a good marker for evaluating the therapeutic efficacy of
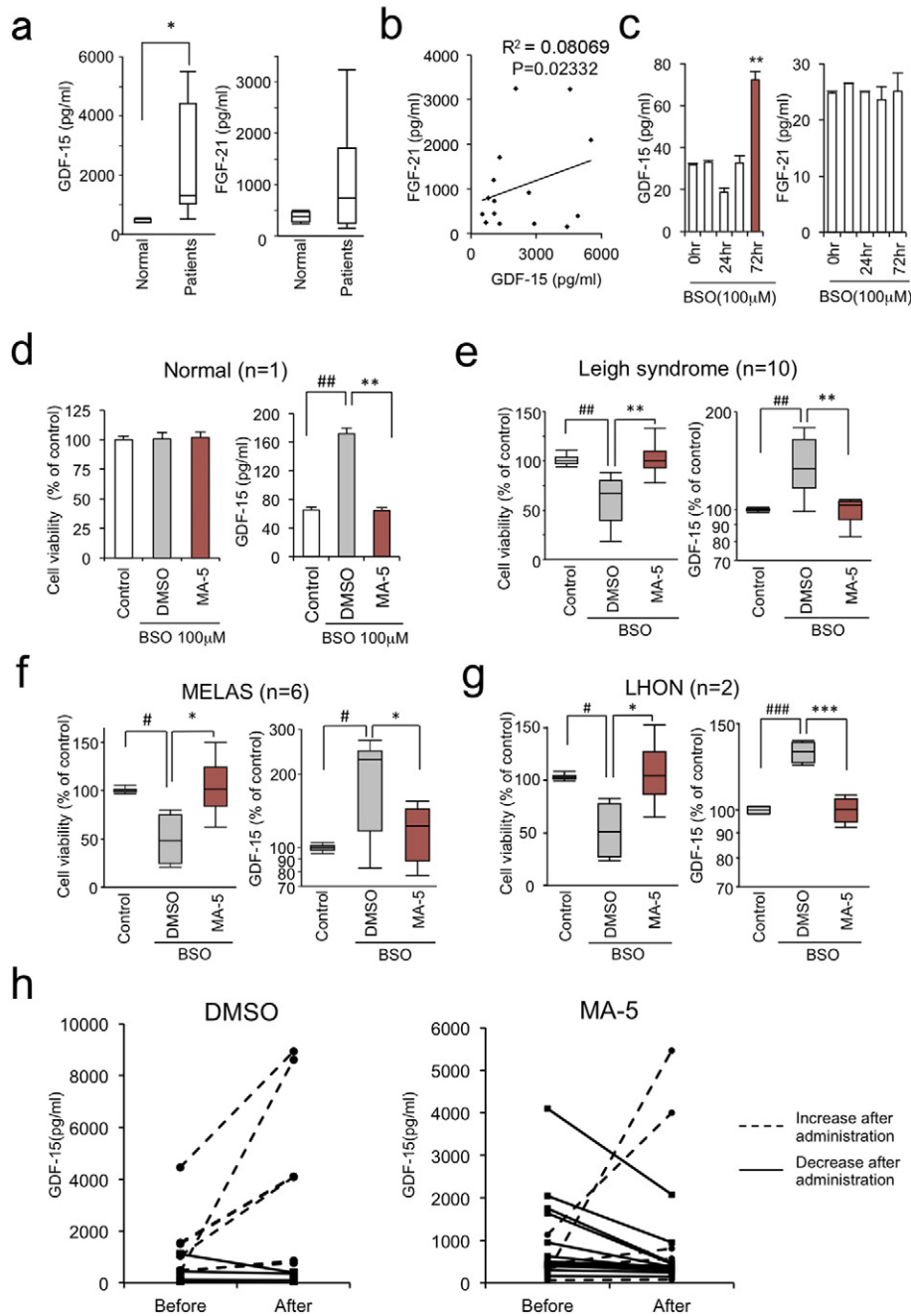
Fig. 2. Measurement of the level of GDF-15 and FGF-21 in patient's serum and in the supernatant of cultured mitochondrial patient's fibroblasts. (a) The level of GDF-15 and FGF-21 in 17 mitochondrial disease patients' serum. **$p < 0.001$ ($p = 0.0082$, non-parametric Wilcoxon rank sum test; $n = 17$). (b) The relationship between GDF-15 and FGF-21 in the mitochondrial disease patients' serum ($n = 17$). (c) GDF-15 and FGF-21 time course assay after BSO treatment in Leigh disease fibroblasts (Case 5 in Table 1) **$p < 0.01$ (unpaired two-tailed Student's *t*-test versus 0 h). The data are expressed as mean ± SEM. The measurement of normal (d), Leigh (e), MELAS (f), and LHON (g) fibroblasts in the cell viability assay (left panel) after 72 h-DMSO application as control and 72 h-MA-5 at 10 μM treatment under 24 h-BSO treatment-induced oxidative stress in each mitochondrial disease. The levels of GDF-15 (right panel) were measured in the same manner in cultured fibroblast medium. #$p < 0.05$, ##$p < 0.01$, ###$p < 0.001$ (two-way ANOVA and Tukey–Kramer test versus Control), *$p < 0.05$, **$p < 0.01$ and ***$p < 0.001$ (two-way ANOVA and Tukey–Kramer test versus BSO + DMSO; normal fibroblast $n = 1$, Leigh syndrome $n = 10$, MELAS $n = 6$ and LHON $n = 2$). Data are expressed as the mean ± SEM. The vertical axis is in logarithmic notation. (h) The level of GDF-15 in Mitomouse with DMSO treatment (left, $n = 11$) and MA-5 (right, $n = 17$), respectively. Note that in MA-5 group, GDF-15 level was significantly decreased ($p = 0.0369$, non-parametric Wilcoxon rank sum test).

MA-5 in vivo given the paucity of diagnostic markers for mitochondrial disease.

3.4. Mitochondrial Bioenergetic Analysis

We next measured the mitochondrial bioenergetic function governing the oxygen consumption rate (OCR) and extra-cellular acidification rate (ECAR) (Pelletier et al., 2014; Rose et al., 2014). The basal and oligomycin-inhibited cellular OCR in the normal and Leigh syndrome fibroblasts were at the same level. After Carbonyl cyanide-*p*-trifluoromethoxyphenylhydrazone (FCCP, a mitochondrial uncoupler) treatment, the OCR values were significantly increased in both, but the increase was appreciably smaller in the Leigh syndrome fibroblasts because of the genetic impairment in ETC activity Fig. 3a, left). The overall ECAR values were appreciably higher in the Leigh syndrome fibroblasts, suggesting that glycolysis was activated to compensate for the genetic impairment in mitochondrial OXPHOS (Fig. 3a, right). In such cells, MA-5 treatment did not affect the FCCP-stimulated OCR

value and ECAR values (Fig. 3b), suggesting that MA-5 may not affect intracellular mitochondrial respiratory activity and glycolysis in Leigh syndrome fibroblasts. These data suggest that MA-5 may not affect intracellular mitochondrial respiratory activity and glycolysis in Leigh syndrome fibroblasts.

To further examine the mitochondrial function, the mitochondrial membrane potential and mitochondrial ROS formation in the fibroblasts were monitored. The mitochondrial membrane potential was not changed by BSO treatment both in normal and Leigh syndrome fibroblasts (Fig. 3c). In addition, MA-5 did not change the mitochondrial membrane potential in both fibroblasts. In contrast, mitochondrial ROS generation was significantly reduced by MA-5 (Fig. 3d). These data further suggest that MA-5 reduces mitochondrial ROS generation independently of the membrane potential.

However, when we measured the ATP levels in Leigh's syndrome (Case 10 in Table 1) and MELAS (Case 15 in Table 1) patient fibroblasts, it would be revealed that the APT level in patient fibroblasts were significantly increased by treatment with MA-5 (Fig. 3e). These results further suggest that MA-5 facilitates mitochondrial ATP production and reduces mitochondrial generation independently of OXPHOS/ETC chemiosmotic machinery (Suzuki et al., 2016).

3.5. MA-5 Increased Supercomplex Formation of ATP Synthase

More than 90% of ATP production is made by OXPHOS. Based on chemiosmotic theory, the movement of ions across an electrochemical potential is able to provide the energy needed to produce ATP (Mitchell, 1961; Pieczenik and Neustadt, 2007). However, as shown in
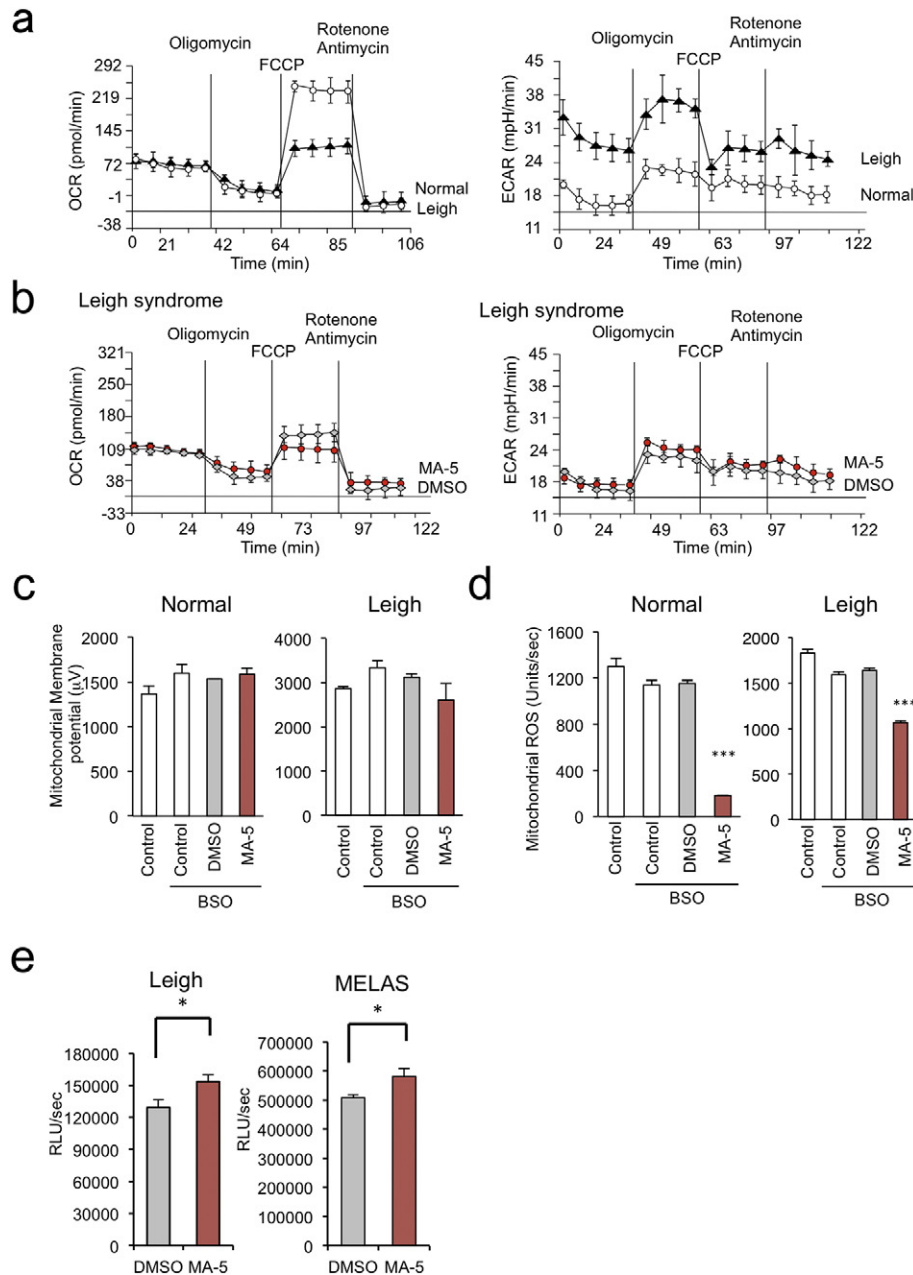

Fig. 3. Effects of MA-5 on mitochondrial respiration. (a) Bioenergetic assay with normal and Leigh syndrome fibroblasts in comparison with OCR (left) and ECAR (right). (b) Bioenergetic assay with fibroblasts from Leigh patient treatment with DMSO or MA-5 (10 μM) in comparison with OCR (left) and ECAR (right). (c) Mitochondrial membrane potentials in normal fibroblast (left) and Leigh syndrome fibroblasts (right). (d) Mitochondrial ROS production was reduced by MA-5-treatment of normal fibroblasts (left) and Leigh syndrome fibroblasts (right) under the oxidative stress induced by BSO-treatment. (e) MA-5 increased the ATP level of fibroblasts of Leigh syndrome (left) and MELAS (right) treated with DMSO and MA-5 (10 μM) for 3 h. *p < 0.01 (unpaired two-tailed Student's t-test versus DMSO).

Fig. 1 and Table 1, MA-5 ameliorated cell death in vitro and in vivo independently of the patient mutations in OXPHOS complex I, IV and ATPase6 that gene mutation that have been found in approximately 20% of people with Leigh syndrome. As we reported, MA-5 completely rescued cell viability compromised by the addition of the ECT inhibitors rotenone (complex I), malonate (complex II), antimycin A (complex III), azide (complex IV) and oligomycin (complex V, F_o part), as well as FCCP (Suzuki et al., 2015). Our data had indicated that MA-5 does not exert its function independently of mitochondrial ETC or the increasing membrane potential. One of the possible mechanisms of action of MA-5 is an effect on the oligomerization of ATP synthase (Suzuki et al., 2016). The oligomerization of ATP synthase is essential for the maintenance of cristae junctions (Habersetzer et al., 2013). In addition, the oligomerization of ATP synthase increases the local pH gradient and membrane potential, and optimizes ATP synthesis without changing the whole mitochondrial membrane potential (Strauss et al., 2008).

To clarify the mechanism by which MA-5 accelerates ATP synthesis, we examined the supercomplex formation of ATP synthase by in-gel visualization of ATP synthesis using clear native-PAGE (CN-PABE). Fig. 4a shows the characteristic "ladder" of the bands representing monomeric, dimeric and multimeric complexes of ATP synthase, and the intensity represents the resulting production of ATP (Strauss et al., 2008). The dimeric and multimeric ATPase complexes formation and ATP production were significantly facilitated by MA-5 ($n = 3$) indicating that MA-5 directly increased ATP production. In addition, increasing the detergent concentration (0.5 to 1% digitonin) resulted in a decrease of the dimer and a corresponding increase in the monomeric form, as reported (Arnold et al., 1998) (Fig. 4a). Western blot analysis also revealed that MA-5 significantly increased the intensity of the dimer band and the higher complexes of the ATP5A compared with the DMSO treated group (Fig. 4b). We also confirm this by AR5B and mitofilin/Mic60 antibodies (Supplementary Fig. S4). The intensity of the dimer band was also decreased and that of the monomer band was increased by the increment of the detergent concentration, confirming that MA-5 facilitates the dimeric formation of ATPase. To compare the intensity of each of the monomer and dimer bands, we further performed SDS-PAGE under a reducing condition and western blotting was performed by VDAC1 as a mitochondrial internal marker to confirm the loading protein level. We found that the intensity of the MA-5-treated dimer bands standardized with VDAC1 was significantly increased compared with the DMSO-treated group, while the intensity of the monomer bands of the MA-5-treated group was not significantly changed compared with the bands of the DMSO-treated group (representing 0.25% digitonin panle, Fig. 4c). These data further confirmed that MA-5 facilitates the dimer formation of ATPase.

It was reported that the oligomerization of ATP synthase depends on the interaction of two subunits of the F_o portion, subunit e (Su e) and subunit g (Su g). These subunits are involved in generating the mitochondrial cristae morphology and the assembly of ATP synthase oligomers, thus controlling mitochondrial biogenesis (Arnold et al., 1998; Bornhovd et al., 2006; Habersetzer et al., 2013). Recently, it was also reported that mitofilin/Mic60 interacts with the Su e and Su g subunits and regulates ATP production (Mun et al., 2010; Rabl et al., 2009). Therefore, we next performed Western blot analyses using blue native PAGE (BN-PAGE, Fig. 4d). Western Blot analysis of BN-PAGE revealed that ATP5A (F_1 α subunit) and ATP5B (F_1 β subunit) were specifically detected at the same molecular sizes as the monomer, dimer and multimer complexes of the ATP synthase, and MA-5 also enhanced the intensity of ATP5A and ATP5B. In addition, Western blot against mitofilin/Mic60, ATP5I (Su e) and ATP5L (Su g) revealed that the bands of the dimer and multimer were also increased by MA-5. These data suggest that MA-5 enhances the supercomplex formation among ATP synthase, mitofilin, Su e and Su g.

To further determine the component of the ATP supercomplex enhanced by MA-5, we examined bands that were increased in intensity by MA-5, digesting them with trypsin and analyzing the peptides with LC/MS/MS. All the bands that were increased in intensity by MA-5 contained ATP5A, ATP5B and mitofilin/Mic60 (Fig. 4e). In Band 1, the complex I components, complex V components and SLC25A5/SLC25A6 proteins were determined. In Band 2, the complex I components, complex V components and SLC25A5 proteins were determined. In Band 3, the complex I components, complex IV component and SLC25A4 proteins were determined. In addition, these complexes contained ADP/ATP carrier 1, 2, 3 (SLC25A4, SLC25A5, SLC25A6, respectively). The mitochondrial ADP/ATP carrier imports ADP from the cytosol and exports ATP from the mitochondrial matrix, which are key transport steps for oxidative phosphorylation and a component of supercomplex (Nuskova et al., 2015). We also examined the protein-protein interaction with mitofilin/Mic60. Proteins bound to Flag-tagged mitofilin/Mic60 were precipitated and examined. As shown in Fig. 4f, flag-tagged mitofilin/Mic60 significantly bound ATP5A and ATP5B as well as ATP/ADP carriers. SAM50, an outer membrane protein, was also precipitated as supercomplex component (Koob and Reichert, 2014) and the mitofilin/mitochondrial inner membrane organizing system (MINOS) complex (Koob and Reichert, 2014), both of which determine cristae morphology.

To further address the supercomplex formation induced by MA-5, change in the size of the ATP synthase complex was examined. In the gel filtration analysis, ATP5A and mitofilin/Mic60 co-migrated as a large protein complex and displayed an apparent molecular weight of approximately 1 MDa (Fig. 4g). The fractions containing ATP5A (upper) and mitofilin/Mic60 (lower) were shifted to the higher fraction size by the application of MA-5. In both, the band intensity of smaller size was decreased by MA-5 treatment compared to DMSO treatment. These results suggest that MA-5 has a potent capacity to assemble into a supercomplex.

3.6. MA-5 Restored Damaged Cristae Morphology

Because the mitochondrial cristae shape determines both respiratory chain supercomplex assembly and respiratory efficiency, and the cristae shape and ATPase dimers are linked to ensure the optimal bioenergetic competence of mitochondria (Paumard et al., 2002), we examined the electron micrograph of fibroblasts from Leigh syndrome patient.

Under stress condition, mitochondrial fission occurs and the reticular mitochondria break into short, round pieces, a process defined as mitochondrial fragmentation. Accordingly, we investigated whether the protective effects of MA-5 are mediated by a prevention of mitochondrial fragmentation. As seen in Fig. 5a, the reticularity of the mitochondrial network was broken into small, round-shaped mitochondrial pieces after BSO exposure. Treatment with MA-5 restored the mitochondrial tubular network in BSO-exposed cells. We measured a cross-sectional area of mitochondria in the patient fibroblasts to determine the effects of BSO exposure on mitochondrial morphology and the degree of mitochondrial network branching. The recovery of the calculated average cross-sectional area was observed to be significant in the MA-5 treated group compared with BSO treatment alone.

The mitochondrial cristae shape also determines both the respiratory chain supercomplex assembly and respiratory efficiency, and the cristae shape and ATPase dimers are linked to ensure the optimal bioenergetic competence of mitochondria (Paumard et al., 2002).

We further examined by electron micrograph of fibroblasts from Leigh syndrome patient (Fig. 5b). The mitochondrial cristae in the patient fibroblasts were enlarged and shortened to the extent that the cristae junctions were loose. On the other hand, MA-5 administration changed the cristae shape to become thinner and longer. The maximal length/width of MA-5 treated mitochondrial cristae was significantly increased compared to the control (Fig. 5b, $p < 0.05$, $n = 100$, see also Supplementary Fig. S4). These data further suggest that MA-5 regulates mitochondrial respiratory efficiency by changing the shape of the cristae in biological membranes.
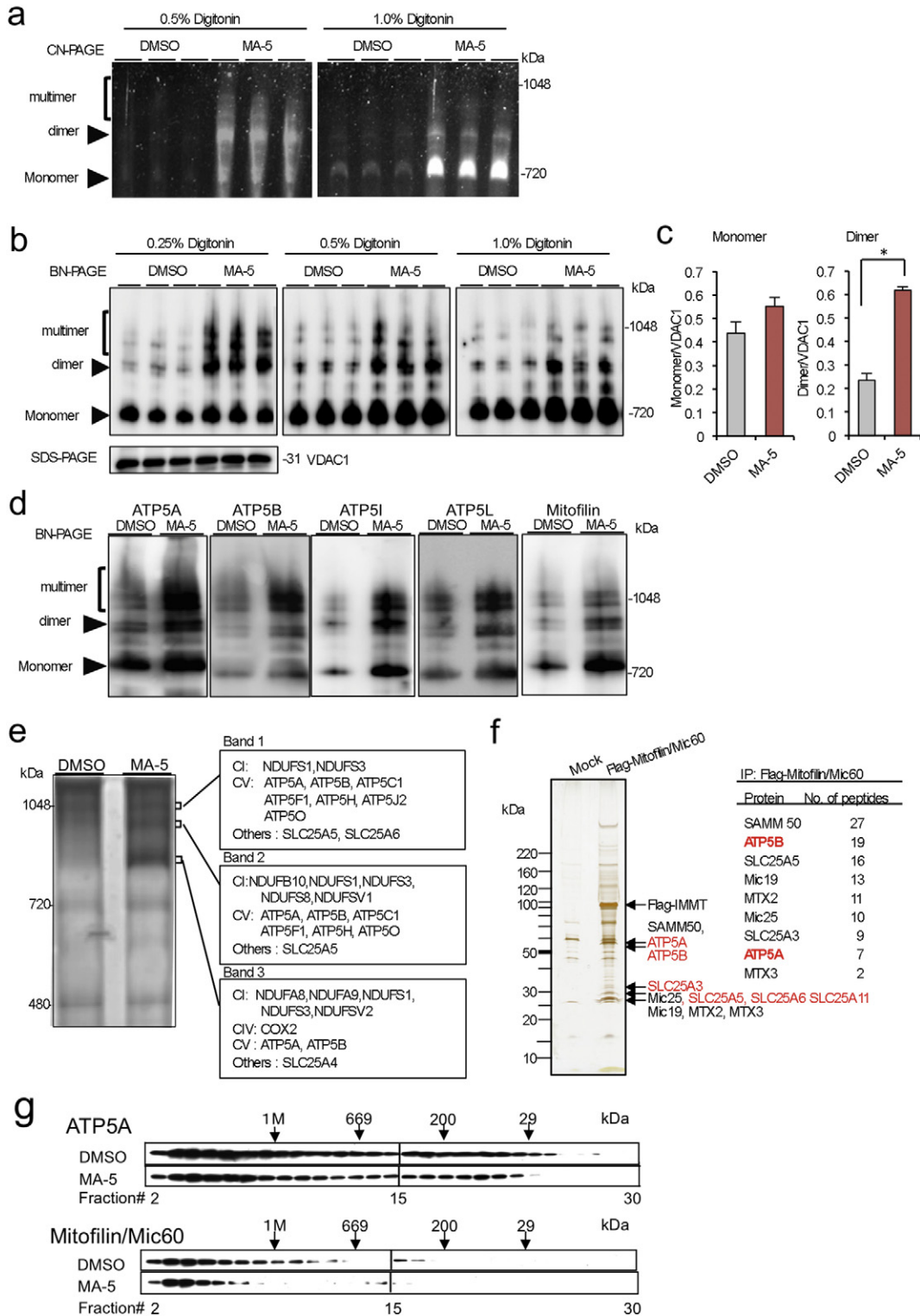
Fig. 4. MA-5 accelerated ATP production with the ATP synthase dimer resulting in supercomplex formation. (a) In gel ATP synthase activity. Native gel of whole, solubilized bovine heart mitochondria with two different concentrations of digitonin (0.5% or 1.0%) stained for ATP synthesis activity. The bands corresponding to the ATP synthase monomer and dimer were indicated by arrowheads. Note that MA-5 increased the intensity of ATPase dimer and multimer formation. (b) Western blotting analysis of Blue-Native gels. The same amounts of isolated mitochondria were treated with three different concentrations of digitonin (0.25%, 0.5% and 1%) and treated with DMSO or MA-5. The resultant protein was electrophoresed and transferred on a membrane. Antibody against ATP5A was used. (c) Comparison with the western blotting densitometric analysis on BN-PAGE representing 0.25% digitonin panle. The monomer (left panel) and dimer (right panel) bands were standardized by VDAC1, which is the loading control on SDS-PAGE. (d) Western blotting analysis of Blue-Native gel treated with DMSO and MA-5 with ATP5A, ATP5B, ATP5I (e), ATP5L (g) and mitofilin/Mic60 antibodies. (e) The LC/MS analysis of the supercomplex components enhanced by MA-5 on BN-PAGE. (f) Putative mitofilin/Mic60-binding proteins identified by affinity chromatography and mass spectrometry (Kanno et al., 2007). (g) Elution profile of MA-5 treatment or non-treatment IMMT and ATP5A on size-exclusion chromatography. MA-5 treatment (10 μM, 1 h) and non-treatment HEC293T cell extracts were separated on a Superose™ 6 (GE Healthcare). Proteins of each fraction were then separated by SDS-PAGE and analyzed by western blotting with an anti-IMMT antibody and anti-ATP5A antibody. After MA-5 treatment, the fractions containing ATP5A (upper) and mitofilin/Mic60 (lower) were shifted to the higher fraction size.
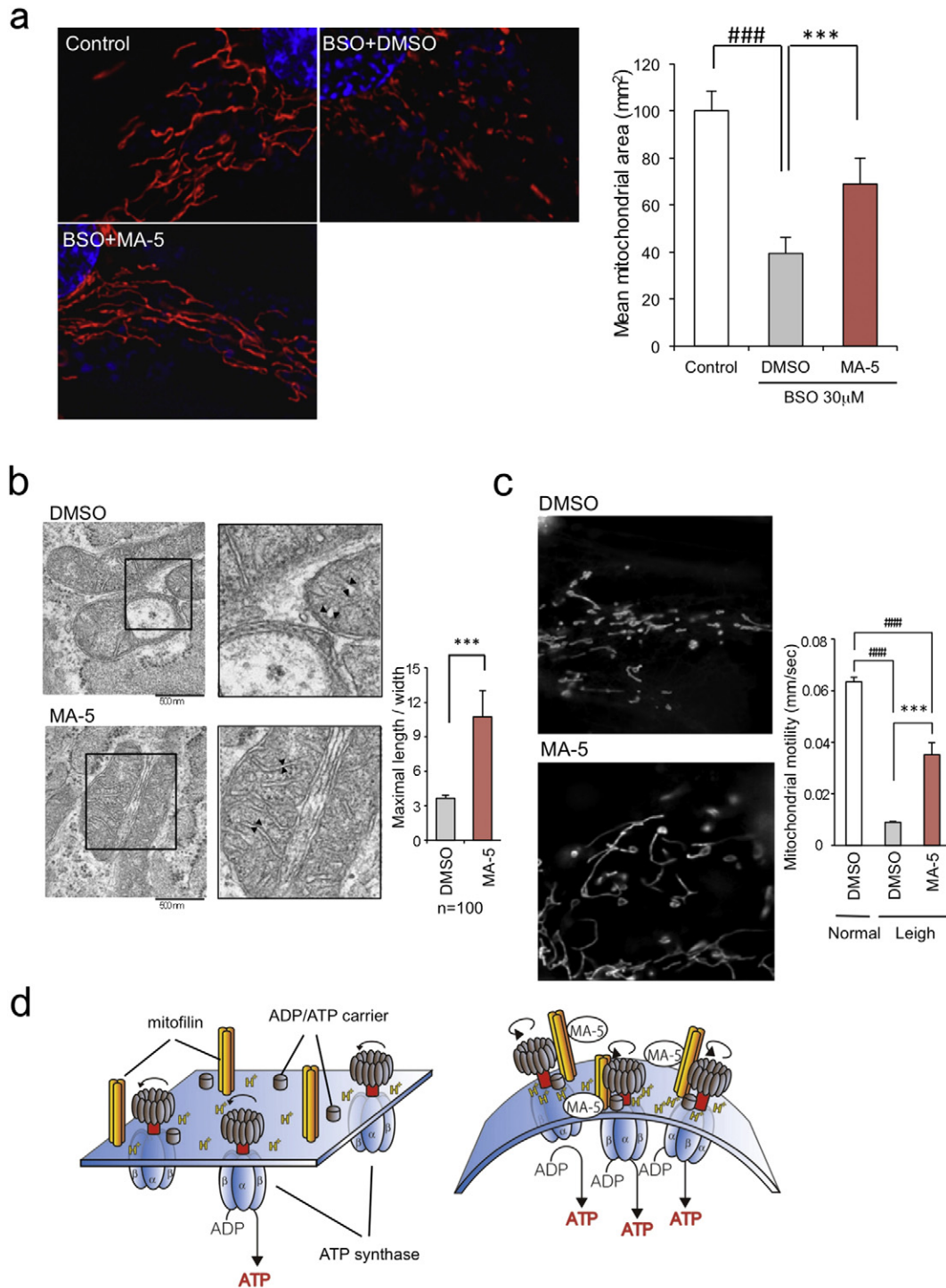
Fig. 5. (a) MA-5 improved mitochondrial fragmentation. The structural change in mitochondria obtained using super resolution microscopic imaging of the control (upper left), BSO + DMSO (upper right) and BSO + MA-5 (lower) fibroblasts (BSO 30 μM, DMSO 0.1% and MA-5 10 μM). ***$p < 0.001$ (unpaired two-tailed Student's t-test versus BSO + DMSO; right graph). (b) MA-5 improved cristae length. Note that the cristae were damaged by BSO and that MA-5 lengthened and tightened the cristae morphology. Arrowhead indicated the cristae. The ratio of the cristae length and width was calculated ($n = 100$). *$p < 0.05$, **$p < 0.01$ and ***$p < 0.001$(two-way ANOVA test versus BSO + DMSO). (c) MA-5 improved mitochondrial movement. Mitochondrial motility of Leigh syndrome fibroblasts (Case 6 in Table 1) with BSO (left, upper) or with MA-5 (left lower) was measured. Note that the mitochondrial motility was significantly increased by MA-5. ***$P < 0.001$ unpaired two-tailed Student's t-test versus normal fibroblast with BSO and Leigh syndrome fibroblast treated with DMSO versus MA-5. (d) Role of the dimerization and oligomerization of the ATP synthase by MA-5. Under a proton-limited condition such as in mitochondrial diseases, destabilization of the ATP synthase complex leads to an increase in fluidity and reduced efficacy of ATP production (Bornhovd et al., 2006) (left panel). MA-5 stimulates the dimerization and oligomerization of the ATP synthase as well as ADP/ATP carrier in cristae formation 5 and the formation of ATP synthase supercomplex may lead to a higher order organization of not only the ATP synthase but also other supracomplexes (Strauss et al., 2008) (right panel). This enforces a strong local curvature on the membrane that act as proton traps, which may lead to effective ATP synthesis.

3.7. Mitochondrial Dynamics

It is well known that the cellular energy state modulates the dynamics of mitochondria (Giedt et al., 2012). Time-lapse imaging by Super-

resolution microscopy revealed that the mitochondrial movement in the Leigh syndrome fibroblasts was significantly slower (0.0090 ± 0.0004 μm/s) compared to normal fibroblasts (0.0633 ± 0.0018 μm/s) (Fig. 5c). MA-5 treatment significantly improved the mitochondrial

mobility in Leigh patient fibroblasts (0.0352 ± 0.0046 μm/s) (live images are on Supplementary Video Data 1 (DMSO) and Video Data 2 (MA-5)). These data further suggest that MA-5 improves mitochondrial morphology and dynamics.

4. Discussion

There were several reports that the dimerization increased ATP synthesis (Davies et al., 2011; Strauss et al., 2008). Recently, it is reported that respiratory supercomplex assemblies increase in response to exercise (Greggio et al., 2017). However, there has been no method to increase the ATP synthase dimer formation as well as supercomplex formation by "chemically".

MA-5 had a cell-protective effect in 24 out of 25 cases (96%) using fibroblasts. Among them, there were 7 genetically identified Leigh syndrome patients in which 3 cases had mutations (in the ND3, 1 case in ATPase6 which mutations have been found approximately 20% of Leigh syndrome (Ma et al., 2013), 2 cases in SURF1 (Tanigawa et al., 2012), and 1 case in NDUFA1 (Uehara et al., 2014) genes. There were 6 patients with MELAS, among which 4 had mutations of *tRNA-Leu*, 1 of *tRNA-Phe* and 1 of *tRNA-Met* (D'Aco et al., 2013). We examined 3 cases of LHON disease in which the mutation was in ND4 (Amati-Bonneau et al., 2009; Lenaers et al., 2012) and 1 case of a DOA patient with an OPA1 gene mutation (Amati-Bonneau et al., 2009). Although the genetic mutations diverged widely in OXPHOS, MA-5 exerted its cell protective effect on almost all of the patients.

How does MA-5 exert an effect on various mitochondrial diseases even when the ETC system is disturbed? ATP production is typically described based on the chemiosmotic theory that the movement of protons across an electrochemical potential difference provides the energy needed to produce ATP (Mitchell, 1961). Although isolated mitochondrial ATP synthase is fully active as a monomer, the ubiquitous occurrence of ATP synthase oligomerization may also play a critical role in the ATP production (Strauss et al., 2008). The MINOS complex was recently reported to maintain mitochondrial architecture and crista junction integrity (Koob and Reichert, 2014). The mitochondrial cristae act as proton traps, and the proton sink of the ATP synthase at the apex of the compartment favors effective ATP synthesis. In addition, the oligomerization of ATP synthase increases the local pH gradient at the apex and optimizes ATP synthesis without changing the mitochondrial membrane potential (Strauss et al., 2008). The oligomerization depends on two subunits of Su e and Su g, with these two subunits involved in generating the assembly of ATP synthase oligomerization and regulating mitochondrial biogenesis (Bornhovd et al., 2006). It was also reported that the mitofilin/Mic60 homolog Fcj1 interacts with the Su e and Su g and affects ATP synthase oligomerization (Mun et al., 2010; Rabl et al., 2009).

Recently, we found that MA-5 targets the mitochondrial protein mitofilin/Mic60 at the crista junction of inner membrane and postulated the possibility that this alters the conformation of the MINOS (Suzuki et al., 2016). This led to the hypothesis that MA-5 may facilitate ATP synthase oligomerization by interacting with the mitofilin, Su e, Su g and ATPase that form the ATPase supercomplex. As shown in Fig. 4a, MA-5 increased not only ATPase activity but also facilitated formation of the ATP synthase monomer, with higher bands indicating active oligomers up to a multimer. Western blot and MS/MS analyses revealed that, not only ATP synthase, but mitofilin/Mic60, Su e, Su g and various ETC components were precipitated by MA-5 (Fig. 4b, c and d). It is reasonable that ECT components were co-precipitated, because respiratory chain complexes are assembled into a supercomplex (Habersetzer et al., 2013). Gel filtration analysis also supported this in that that MA-5 facilitated the shift of ATP synthase- and mitofilin/Mic60-inclusion bands to the higher molecular weight (Fig. 4f). The EM further revealed that MA-5 change the structural shape of the cristae, and this may be reflected in changes in the shape and dynamics of mitochondria (Fig. 5a–c). Therefore, MA-5 may facilitate supercomplex formation and result in the maintenance of ATPase and MINOS complex integrity "chemically". This supercomplex formation of ATP synthase by MA-5 enables ATP generation without any change in the membrane potential and is independent of damaged ETC.

Our theory of ATP production does not contradict the chemiosmotic theory. However, under proton-limited conditions or genetic mutation has occurred in ETC genes, the mitochondrial cristae modification and supercomplex formation by MA-5 should prove useful for generating the local proton gradient and producing ATP without changing the membrane potential (graphic summary in Fig. 5d), without generating mitochondrial ROS. It is also reported that supercomplex prevents the excessive ROS formation from the mitochondria (Maranzana et al., 2013). Thus, MA-5 has the potential to treat mitochondrial patients with genetic mutations within various OXPHOS components, if F_1F_0 portion of ATP synthase itself is intact, as in the cases we studied.

Our data also show the potential diagnostic use of GDF-15, which will be utilized in a forthcoming MA-5 clinical trial. There are several discussion on which is diagnostic better between GDF-15 and FGF-21. Lehtonen et al. reported that FGF-21 is a specific biomarker for muscle-manifesting defects of mitochondrial translation, the most common causes of mitochondrial disease. However, GDF-15 was increased also in a wide range of non-mitochondrial conditions (Lehtonen et al., 2016). On the other hand, Davis et al. reported that the serum GDF-15 measurement may be more broadly specific for mitochondrial disease than for muscle manifesting mitochondrial disease, in contrast to FGF-21 (Davis et al., 2016). GDF-15 concentrations were high in a variety of severe disorders. However, as also mentioned by Lehtonen et al., in Leigh syndrome or Leber hereditary optic atrophy, the FGF-21 can remain low (Lehtonen et al., 2016). Because Mitomouse is a mouse model for Leigh syndrome (Nakada et al., 2001), the difference of model may be the cause of our difference between GDF-15 and FGF-21. Although GDF-15 is one of a candidate marker for mitochondrial damage, further experiments will be necessary to find a suitable marker for predicting the clinical effect of MA-5 in vivo and for further clinical study.

Finally, it is recently reported that respiratory supercomplex assemblies increase in response to exercise (Greggio et al., 2017). Our drug MA-5 is an alternative exercise mimetics to increase the formation of ATP synthase dimer and supercomplex formation chemically, important on health and performance. It will be helpful not only mitochondrial disease but also other mitochondria-related metabolic disorders such as diabetes, diabetic nephropathy, cardiomyopathy, longevity etc.

Supplementary data to this article can be found online at http://dx.doi.org/10.1016/j.ebiom.2017.05.016.

Conflicts of Interest

None.

Author Contributions

T.S., S.K., H.O., K.N., K.-I.H., S.-I.K. and T.A. designed the experiment. K.-I.H. for in-house chemical syntheses. A.W. performed skin biopsy from mitochondrial patients. H.Y. for performed binding assay. M.K., T.S., A.M., Y.O., K.S., F.N., Y.M., T.K. H-J.H. and T.M. performed mitochondrial analyses. M.O., E.O. and K.N. performed mice experiments. E.M., H.S., Y.A., K.K. and C.S. performed cell culture and viability experiments. O.O. performed heteroplasmy analysis by NGS. D.S. and A.H. advised for

statistical analysis of experimental data. K.N., M.T., Y.O., S.A., T.Y., S.K., S.I., K.N., H.O., S.I. and T.A. for discussion.

References

Amati-Bonneau, P., Milea, D., Bonneau, D., Chevrollier, A., Ferre, M., Guillet, V., Gueguen, N., Loiseau, D., de Crescenzo, M.A., Verny, C., et al., 2009. OPA1-associated disorders: phenotypes and pathophysiology. Int. J. Biochem. Cell Biol. 41, 1855–1865.

Arnold, I., Pfeiffer, K., Neupert, W., Stuart, R.A., Schagger, H., 1998. Yeast mitochondrial F1F0-ATP synthase exists as a dimer: identification of three dimer-specific subunits. EMBO J. 17, 7170–7178.

Avula, S., Parikh, S., Demarest, S., Kurz, J., Gropman, A., 2014. Treatment of mitochondrial disorders. Curr. Treat. Options Neurol. 16, 292.

Bornhovd, C., Vogel, F., Neupert, W., Reichert, A.S., 2006. Mitochondrial membrane potential is dependent on the oligomeric state of F1F0-ATP synthase supracomplexes. J. Biol. Chem. 281, 13990–13998.

D'Aco, K.E., Manno, M., Clarke, C., Ganesh, J., Meyers, K.E., Sondheimer, N., 2013. Mitochondrial tRNA(Phe) mutation as a cause of end-stage renal disease in childhood. Pediatr. Nephrol. 28, 515–519.

Davies, K.M., Strauss, M., Daum, B., Kief, J.H., Osiewacz, H.D., Rycovska, A., Zickermann, V., Kuhlbrandt, W., 2011. Macromolecular organization of ATP synthase and complex I in whole mitochondria. Proc. Natl. Acad. Sci. U. S. A. 108, 14121–14126.

Davis, R.L., Liang, C., Sue, C.M., 2016. A comparison of current serum biomarkers as diagnostic indicators of mitochondrial diseases. Neurology 86, 2010–2015.

Enns, G.M., Kinsman, S.L., Perlman, S.L., Spicer, K.M., Abdenur, J.E., Cohen, B.H., Amagata, A., Barnes, A., Kheifets, V., Shrader, W.D., et al., 2012. Initial experience in the treatment of inherited mitochondrial disease with EPI-743. Mol. Genet. Metab. 105, 91–102.

Fujita, Y., Ito, M., Kojima, T., Yatsuga, S., Koga, Y., Tanaka, M., 2014. GDF15 is a novel biomarker to evaluate efficacy of pyruvate therapy for mitochondrial diseases. Mitochondrion 20C, 34–42.

Giedt, R.J., Pfeiffer, D.R., Matzavinos, A., Kao, C.Y., Alevriadou, B.R., 2012. Mitochondrial dynamics and motility inside living vascular endothelial cells: role of bioenergetics. Ann. Biomed. Eng. 40, 1903–1916.

Gorman, G.S., Chinnery, P.F., DiMauro, S., Hirano, M., Koga, Y., McFarland, R., Suomalainen, A., Thorburn, D.R., Zeviani, M., Turnbull, D.M., 2016. Mitochondrial diseases. Nat. Rev. Dis. Primers 2, 16080.

Greggio, C., Jha, P., Kulkarni, S.S., Lagarrigue, S., Broskey, N.T., Boutant, M., Wang, X., Conde Alonso, S., Ofori, E., Auwerx, J., et al., 2017. Enhanced respiratory chain supercomplex formation in response to exercise in human skeletal muscle. Cell Metab. 25, 301–311.

Habersetzer, J., Ziani, W., Larrieu, I., Stines-Chaumeil, C., Giraud, M.F., Brethes, D., Dautant, A., Paumard, P., 2013. ATP synthase oligomerization: from the enzyme models to the mitochondrial morphology. Int. J. Biochem. Cell Biol. 45, 99–105.

Hurko, O., 2013. Drug development for rare mitochondrial disorders. Neurotherapeutics 10, 286–306.

Kanno, S., Kuzuoka, H., Sasao, S., Hong, Z., Lan, L., Nakajima, S., Yasui, A., 2007. A novel human AP endonuclease with conserved zinc-finger-like motifs involved in DNA strand break responses. EMBO J. 26, 2094–2103.

Koob, S., Reichert, A.S., 2014. Novel intracellular functions of apolipoproteins: the ApoO protein family as constituents of the Mitofilin/MINOS complex determines cristae morphology in mitochondria. Biol. Chem. 395, 285–296.

Koopman, W.J., Willems, P.H., Smeitink, J.A., 2012. Monogenic mitochondrial disorders. N. Engl. J. Med. 366, 1132–1141.

Kumari, S., Mehta, S.L., Milledge, G.Z., Huang, X., Li, H., Li, P.A., 2016. Ubisol-Q10 prevents glutamate-induced cell death by blocking mitochondrial fragmentation and permeability transition pore opening. Int. J. Biol. Sci. 12, 688–700.

Lehtonen, J.M., Forsstrom, S., Bottani, E., Viscomi, C., Baris, O.R., Isoniemi, H., Hockerstedt, K., Osterlund, P., Hurme, M., Jylhava, J., et al., 2016. FGF21 is a biomarker for mitochondrial translation and mtDNA maintenance disorders. Neurology 87, 2290–2299.

Lenaers, G., Hamel, C., Delettre, C., Amati-Bonneau, P., Procaccio, V., Bonneau, D., Reynier, P., Milea, D., 2012. Dominant optic atrophy. Orphanet. J. Rare Dis. 7, 46.

Ma, Y.Y., Wu, T.F., Liu, Y.P., Wang, Q., Song, J.Q., Li, X.Y., Shi, X.Y., Zhang, W.N., Zhao, M., Hu, L.Y., et al., 2013. Genetic and biochemical findings in Chinese children with Leigh syndrome. J. Clin. Neurosci. 20, 1591–1594.

Maranzana, E., Barbero, G., Falasca, A.I., Lenaz, G., Genova, M.L., 2013. Mitochondrial respiratory supercomplex association limits production of reactive oxygen species from complex I. Antioxid. Redox Signal. 19, 1469–1480.

Mitchell, P., 1961. Coupling of phosphorylation to electron and hydrogen transfer by a chemi-osmotic type of mechanism. Nature 191, 144–148.

Mun, J.Y., Lee, T.H., Kim, J.H., Yoo, B.H., Bahk, Y.Y., Koo, H.S., Han, S.S., 2010. Caenorhabditis elegans mitofilin homologs control the morphology of mitochondrial cristae and influence reproduction and physiology. J. Cell. Physiol. 224, 748–756.

Nakada, K., Inoue, K., Ono, T., Isobe, K., Ogura, A., Goto, Y.I., Nonaka, I., Hayashi, J.I., 2001. Inter-mitochondrial complementation: mitochondria-specific system preventing mice from expression of disease phenotypes by mutant mtDNA. Nat. Med. 7, 934–940.

Nakayama, M., Oda, H., Nakagawa, K., Yasumi, T., Kawai, T., Izawa, K., Nishikomori, R., Heike, T., Ohara, O., 2017. Accurate clinical genetic testing for autoinflammatory diseases using the next-generation sequencing platform MiSeq. Biochem. Biophys. Reports 9, 146–152.

Nuskova, H., Mracek, T., Mikulova, T., Vrbacky, M., Kovarova, N., Kovalcikova, J., Pecina, P., Houstek, J., 2015. Mitochondrial ATP synthasome: expression and structural interaction of its components. Biochem. Biophys. Res. Commun. 464, 787–793.

Ogata, M., Ota, Y., Nanno, M., Suzuki, R., Itoh, T., 2015. Autocrine DNA fragmentation of intra-epithelial lymphocytes (IELs) in mouse small intestine. Cell Tissue Res. 361, 799–810.

Paumard, P., Vaillier, J., Coulary, B., Schaeffer, J., Soubannier, V., Mueller, D.M., Brethes, D., di Rago, J.P., Velours, J., 2002. The ATP synthase is involved in generating mitochondrial cristae morphology. EMBO J. 21, 221–230.

Pelletier, M., Billingham, L.K., Ramaswamy, M., Siegel, R.M., 2014. Extracellular flux analysis to monitor glycolytic rates and mitochondrial oxygen consumption. Methods Enzymol. 542, 125–149.

Pieczenik, S.R., Neustadt, J., 2007. Mitochondrial dysfunction and molecular pathways of disease. Exp. Mol. Pathol. 83, 84–92.

Rabl, R., Soubannier, V., Scholz, R., Vogel, F., Mendl, N., Vasiljev-Neumeyer, A., Korner, C., Jagasia, R., Keil, T., Baumeister, W., et al., 2009. Formation of cristae and crista junctions in mitochondria depends on antagonism between Fcj1 and Su e/g. J. Cell Biol. 185, 1047–1063.

Rose, S., Frye, R.E., Slattery, J., Wynne, R., Tippett, M., Pavliv, O., Melnyk, S., James, S.J., 2014. Oxidative stress induces mitochondrial dysfunction in a subset of autism lymphoblastoid cell lines in a well-matched case control cohort. PLoS One 9, e85436.

Schapira, A.H.V., 2012. Mitochondrial diseases. Lancet 379, 1825–1834.

Shimbo, H., Takagi, M., Okuda, M., Tsuyusaki, Y., Takano, K., Iai, M., Yamashita, S., Murayama, K., Ohtake, A., Goto, Y.I., et al., 2014. A rapid screening with direct sequencing from blood samples for the diagnosis of Leigh syndrome. Mol. Genet. Metab. Rep. 1, 133–138.

Strauss, M., Hofhaus, G., Schroder, R.R., Kuhlbrandt, W., 2008. Dimer ribbons of ATP synthase shape the inner mitochondrial membrane. EMBO J. 27, 1154–1160.

Suomalainen, A., Elo, J.M., Pietiläinen, K.H., Hakonen, A.H., Sevastianova, K., Korpela, M., Isohanni, P., Marjavaara, S.K., Tyni, T., Kiuru-Enari, S., et al., 2011. FGF-21 as a biomarker for muscle-manifesting mitochondrial respiratory chain deficiencies: a diagnostic study. Lancet Neurol. 10, 806–818.

Suzuki, T., Yamaguchi, H., Kikusato, M., Matsuhashi, T., Matsuo, A., Sato, T., Oba, Y., Watanabe, S., Minaki, D., Saigusa, D., et al., 2015. Mitochonic acid 5 (MA-5), a derivative of the plant hormone indole-3-acetic acid, improves survival of fibroblasts from patients with mitochondrial diseases. Tohoku J. Exp. Med. 236, 225–232.

Suzuki, T., Yamaguchi, H., Kikusato, M., Hashizume, O., Nagatoishi, S., Matsuo, A., Sato, T., Kudo, T., Matsuhashi, T., Murayama, K., et al., 2016. Mitochonic acid 5 binds mitochondria and ameliorates renal tubular and cardiac myocyte damage. J. Am. Soc. Nephrol. 27, 1925–1932.

Tanigawa, J., Kaneko, K., Honda, M., Harashima, H., Murayama, K., Wada, T., Takano, K., Iai, M., Yamashita, S., Shimbo, H., et al., 2012. Two Japanese patients with Leigh syndrome caused by novel SURF1 mutations. Brain Dev. 34, 861–865.

Uehara, N., Mori, M., Tokuzawa, Y., Mizuno, Y., Tamaru, S., Kohda, M., Moriyama, Y., Nakachi, Y., Matoba, N., Sakai, T., et al., 2014. New MT-ND6 and NDUFA1 mutations in mitochondrial respiratory chain disorders. Ann. Clin. Transl. Neurol. 1, 361–369.

Vafai, S.B., Mootha, V.K., 2012. Mitochondrial disorders as windows into an ancient organelle. Nature 491, 374–383.

Yatsuga, S., Fujita, Y., Ishii, A., Fukumoto, Y., Arahata, H., Kakuma, T., Kojima, T., Ito, M., Tanaka, M., Saiki, R., et al., 2015. Growth differentiation factor 15 as a useful biomarker for mitochondrial disorders. Ann. Neurol. 78, 814–823.